Science Arts & Métiers (SAM)

is an open access repository that collects the work of Arts et Métiers Institute of Technology researchers and makes it freely available over the web where possible.

This is an author-deposited version published in: https://sam.ensam.eu
Handle ID: .http://hdl.handle.net/10985/20160

To cite this version :

Ahmed KTARI, A ABDELKEFI, N GUERMAZI, P MALECOT, N BOUDEAU - Numerical investigation of plastic flow and residual stresses generated in hydroformed tubes - Proceedings of the Institution of Mechanical Engineers, Part L: Journal of Materials: Design and Applications p.146442072198974 - 2021

Any correspondence concerning this service should be sent to the repository Administrator : scienceouverte@ensam.eu

Arts et Métiers Institute of Technology

Check for updates

Original article

Institution of MECHANICAL ENGINEERS
Journal of MATERIALS: DESIGN AND APPLICATIONS

Proc IMechE Part L:
J Materials: Design and Applications
0(0) 1–12
© IMechE 2021
Article reuse guidelines:
sagepub.com/journals-permissions
DOI: 10.1177/14644207219897 46
journals.sagepub.com/home/pil
SAGE

Numerical investigation of plastic flow and residual stresses generated in hydroformed tubes

A Ktari[1,2], A Abdelkefi[3], N Guermazi[1], P Malecot[4] and N Boudeau[4]

Abstract

During tube hydroforming process, the friction conditions between the tube and the die have a great importance on the material plastic flow and the distribution of residual stresses of the final component. Indeed, a three-dimensional finite element model of a tube hydroforming process in the case of square section die has been performed, using dynamic and static approaches, to study the effect of the friction conditions on both plastic flow and residual stresses induced by the process. First, a comparative study between numerical and experimental results has been carried out to validate the finite element model. After that, various coefficients of friction were considered to study their effect on the thinning phenomenon and the residual stresses distribution. Different points have been retained from this study. The thinning is located in the transition zone cited between the straight wall and the corner zones of hydroformed tube due to the die–tube contact conditions changes during the process. In addition, it is clear that both die–tube friction conditions and the tube bending effects, which occurs respectively in the tube straight wall and corner zones, are the principal causes of the obtained residual stresses distribution along the tube cross-section.

Keywords

Hydroforming, finite elements analysis, friction coefficient, stick/slip contact, residual stress

Date received: 20 October 2020; accepted: 5 January 2021

Introduction

Cost reduction and product improvement has always been among the main goals of advanced metal-forming processes. Thus, several researches have been developed to study the metal-forming processes. During the last decades, various industries pay a great attention to tube hydroforming (THF) process and, therefore, it has become one of the most commonly used in metal-forming processes and the leader in automobile industry.[1] Moreover, this process was implanted in aerospace industry due to its capability of manufacturing complex shapes with a simpler technique than accustomed stamping, forging, and welding processes.[2] Indeed, the THF is a metal-forming process, which consists of deforming plastically a tube in a shape die with the conjunction of the internal pressure only. In this case, we talk about pure expansion as a single-step THF process. Moreover, an axial compressive force can be applied in the extremities in order to facilitate the flow of material and thus a better distribution of deformation.[3]

The THF process presents many advantages including weight reduction, lower tooling cost, and low spring-back. Nevertheless, it presents some drawbacks as well as costly equipment and lack of knowledge bases for manufacturing process and tool design. During a THF operation, several defects may occur in the final workpiece like the plastic instability. For the main failure modes, we find bursting, wrinkling, and buckling. However, there exist other kinds of defaults like sealing problems and bad thickness distribution. These defects are mainly associated to the THF process parameters, tooling, and tube material.[4] Among these parameters, we can mention loading paths,[5] die

[1]Laboratoire de Génie des Matériaux et Environnement (LGME), ENIS, Université de Sfax, Tunisia
[2]MSMP-EA7350, Arts et Métiers ParisTech, Aix-en-Provence, France
[3]Institut National des Sciences Appliquées de Rennes, LGCGM, Rennes, France
[4]UBFC/CNRS-UMR9174/UFC/ENSMM/UTBM, FEMTO-ST, Department of Applied Mechanics, Besançon, France

Corresponding author:
A Ktari, Laboratoire de Génie des Matériaux et Environnement (LGME), ENIS, Université de Sfax, BP 1173-3038, Sfax 3038, Tunisia.
Email: ahmed.ktari@enis.tn

design,[6] friction at the tube–die interface,[7] and material properties.[8]

The thickness distribution of hydroformed tube depends on several parameters, especially those related to the material's plastic behavior such as the strain-hardening exponent and the anisotropy coefficients. Fuchizawa[9] studied the effect of strain hardening coefficient "n". The obtained results showed that, the pressure needed to bulge a certain height decreases and that the thickness distribution becomes more uniform when n increases. In this context, Khalfallah et al.[10] have investigated the effect of two anisotropy Lankford coefficients R_0 and R_{90} according to the axial and circumferential directions, respectively. The result reveals that R_0 coefficient has a nonsignificant effect on the thickness distribution especially in the guiding zone. However, a high value of anisotropy coefficient R_{90} improves considerably the thickness uniformity of the tube wall.

In order to investigate the effect of coefficient of friction (COF) on the thickness distribution, Khalfallah et al.[10] have carried out a set of finite element analysis for different COF values. Thus, they prove that the increase of COF reduces the thickness distribution uniformity especially in the expansion zone. Hwang and Chen[11] developed a mathematical model, taking into account the sliding friction between the hydroformed tube and the tool, to estimate the pressure needed to form a tube in a square cross-section die and to predict the thickness distribution in the final structure. The authors have found that a good lubrication can reduce any risk of buckling and wrinkling. Geiger et al.[12] used a specific lubricant to improve the formability in THF by decrease of friction. Indeed, the lubrication helps to soften the contact and permits the sliding between the tube and the tool surface. Fiorentino et al.[13] experimentally studied the effect of the lubrication in T-shape section. The experimental test has been performed with pin-on-disk test. In fact, the use of different lubricants leads to deduce various friction coefficients and therefore their effect on the final part as well as the bulge height and thickness distribution. Yuan et al.[14] achieved experimental tests for different geometries as square and rectangular shapes. The numerical results obtained with the dynamic-explicit finite element (FE) code LS-DYNA have shown the validity of the models. The authors have shown that the thickness is maximal at the middle of the flat part of the shaped tube, while thinning occurs in the transition zone between the flat part and the radius of the formed tube.

Several authors have also studied and investigated the effect of the process parameters as internal pressure on the THF process. Chen et al.[15] proposed a theoretical model, which concerns the relationship between the corner radius and the pressure bulge. Numerical studies correlate well with the analytical model. Indeed, when the hydraulic pressure increases the corner radius decreases. Nikhare et al.[16] studied the effect of the high and low pressure in the hydroforming process through numerical simulation. In fact, the thinning is more important in the high-pressure THF than in the low-pressure THF. The stress and the thinning without friction is less than with friction for the test with high pressure.

In view of the foregoing section, it is clear that THF process in a square section die is widely studied in literature. However, the effect of the friction on plastic strain and residual stresses and its correlation with mechanics involved in hydroforming is not well studied. The residual stresses' prediction generated on hydroformed tube seems to be very important since they can influence the result of a later process step[17] and can affect the structure lifetime in service.[18] As a result, the present paper aims to study the effect of the COF and relative die–tube slip distribution on the tube thinning and residual stresses distribution, and investigate the relationship between the plastic flow and the die–tube contact condition during the studied THF process.

Material and techniques

Studied material

In the present work, the studied workpiece is an extruded tube made of deoxidized copper (Cu-DHP),[19] and manufactured by Wieland Group according to the NF EN 1057 standard. According to the specification, the outside mean diameter of the tube is 35 mm and the average thickness is 0.9 mm. The material properties parameters are identified using free bulge tests. The hydraulic bulge test is widely used for determining the strain-hardening properties of sheet materials in biaxial tension.[20] This test consists of a deformation of a metal tubular specimen with internal pressure until bursting occurs. The strains in hydroforming process are normally larger than the uniform strain range obtained by the conventional uniaxial tensile test. Hence, the bulge test can better describe the plastic properties of a sheet at large strain.[21] By measuring the internal pressure and the tube deformation, a set of mechanical properties data can be obtained (i.e. the internal hydraulic pressure and the maximum bulge height are monitored). Then, post-processing with the Boudeau and Malécot model[22] allowed for the hardening curve (Figure 1). Here, Swift's law was considered according to equation (1), where σ and ε represent the equivalent stress and strain respectively and Swift's parameters (ε_o, K, and n) determined based on the hardening curve (Table 1)

$$\sigma = k(\varepsilon_0 + \varepsilon)^n \quad (1)$$

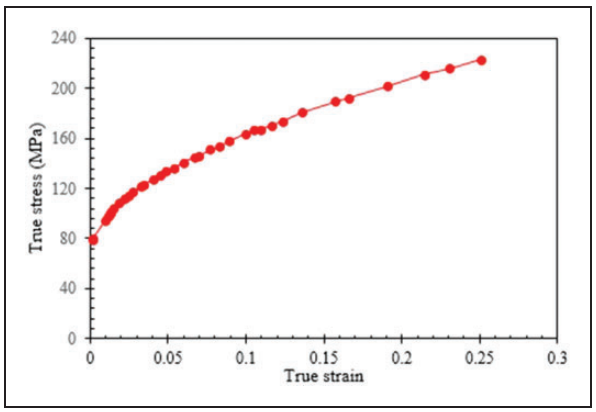

Figure 1. True stress–strain curve of deoxidized copper (Cu-DHP) at room temperature.

Tube hydroforming in a square section die

In order to carry out the THF in a square section die, a modular tool in closed die has been considered and a hydraulic press, with a capacity of 150 MPa, has been used. All the THF process parameters are summarized in Table 2. This test consists of deforming tube with the effect of internal pressure by means of fluid (Figure 2(a)). At the beginning of the test, some parameters, such as (i) the maximal internal pressure, (ii) the sealing force that ensures the clamping of the tube ends, and (iii) the position of the displacement sensors, which are made in order to capture the evolution of the internal pressure during the test, must be adjusted. During the THF in a square section die, several experiments were performed under different lubrication conditions in order to study their effect on the tube formability and then on residual stresses that can be generated after the tube spring-back. The different samples obtained after the spring-back were cut using the wire electrical discharge machining process to avoid additional deformations and to obtain precise contours (Figure 2(b)). From these tube sections, the outer and inner profiles are measured with a contactless metrology machine (Werth IP 250) working with an image outline analysis. The machine automatically followed the sample's profile and acquired a cloud of points. For each part of the hydroformed tube, the inner and outer profiles were measured taking into account an average of 60,000 points. The collected data were analyzed with an original program to determine the thickness repartition along the profile with a repeatability of $\pm 1\,\mu m$.[19] For more details about the experimental procedure, see Abdelkefi et al.[19]

Three-dimensional FE modeling of the problem

In order to model the THF process and to guarantee an efficient and accurate computation, many key techniques need to be considered, such as geometry modeling, definition of material properties, assembling, treating of contact boundary conditions, and mesh.[23] In this study, two steps were defined to simulate the THF process during loading and unloading phases. Since the implicit methods can be extremely time-consuming when solving dynamic and nonlinear problems with a severe die–workpiece contact conditions, the explicit simulation schema was chosen for the loading stage (step duration = 0.01 s). However, since the spring-back process, in the unloading stage, involves only mild nonlinearities and no die–workpiece contact, the implicit schema was selected. This combination of explicit forming and implicit spring-back simulations has been widely applied by researchers to predict residual stresses in metal-forming processes by the use of numerical simulations.[24]

Table 1. Mechanical properties of Cu-DHP material used in FE simulation.

Materials parameters	Value
Density ρ (tonne/mm^3)	8.49×10^{-9}
Young's modulus, E (GPa)	132
Poisson's ratio (υ)	0.34
Yield stress (MPa)	80
Elongation at break (A%)	19
Initial strain, ε_0	7.5×10^{-3}
Hardening coefficient, K (MPa)	442
Hardening exponent, n	0.349

Table 2. The tube THF process parameters.

Process parameters	Values
Die corner radius	5 mm
Square die side	35 mm
Length of tube	250 mm
Thickness of tube	0.9 mm
Internal pressure	280 bar

Tool geometry and mesh

In this section, the FE modeling of THF process in a square section die is carried out. In view of the problem symmetry (geometry, material, load, and boundary conditions), only one eighth of the problem is modeled (Figure 3(a)). The tube is defined as a deformable body with a thickness of 0.9 mm (i.e. the initial cross-section is assumed to be perfectly circular and the initial thickness is uniform) while the die is modeled as a discrete rigid body. The die and the tube were meshed using respectively R3D4 (a four-node 3D bilinear rigid quadrilateral) and C3D8R (a eight-node linear brick, reduced integration, hourglass control) elements on both explicit and implicit computations[23] (Figure 3(b)). The tube was divided into four layers in the thickness direction in order to avoid hourglassing[25] and a mesh refinement is carried out near to the die square section side in order to increase the analysis accuracy. The generated FE

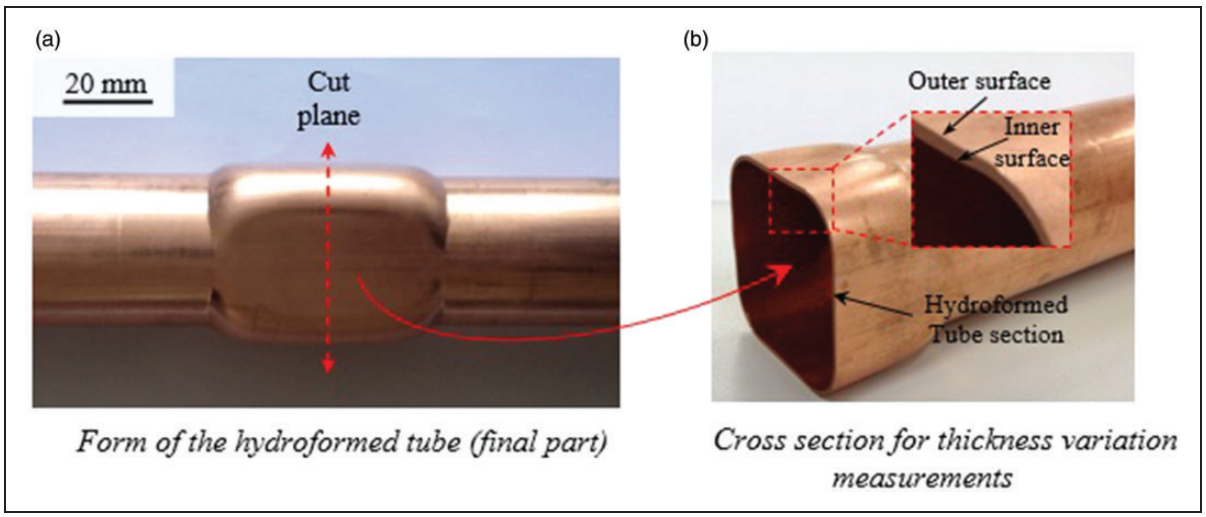

Figure 2. Tube after expansion in a square section die ($P = 28$ MPa).

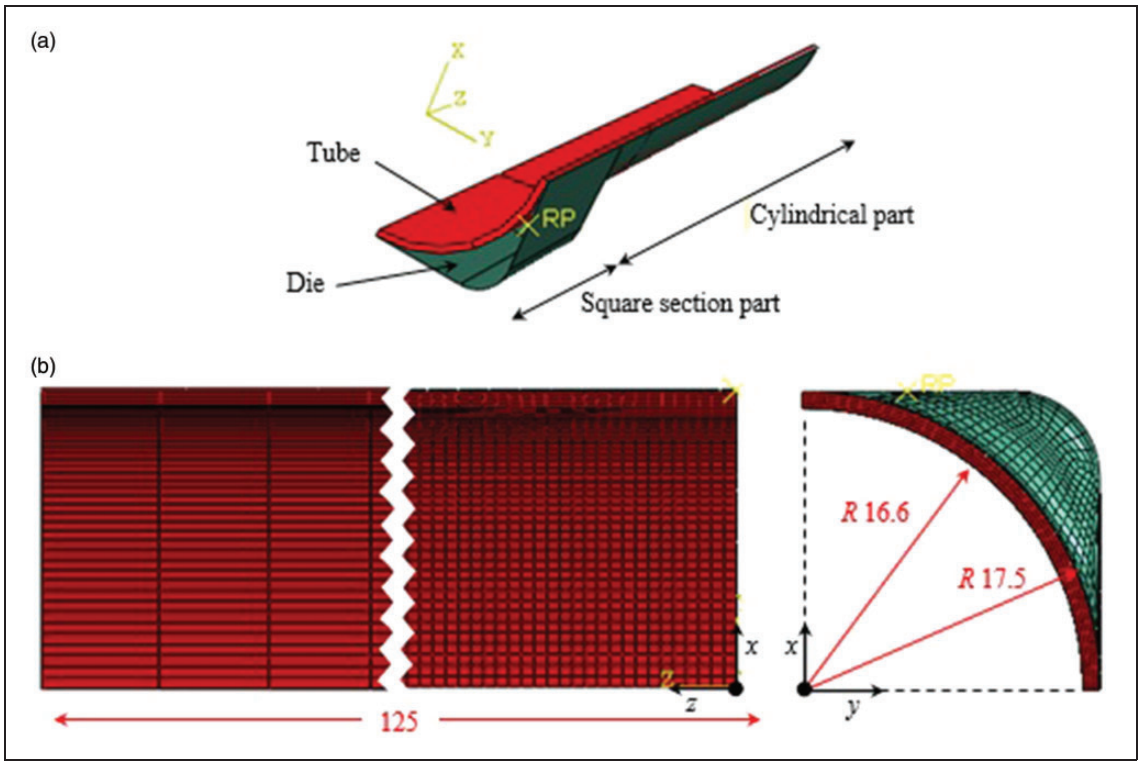

Figure 3. 3D-FE model of a THF process in a square section die: (a) one-eighth of the model; (b) mesh and dimensions (in mm).

mesh includes 14,968 elements, which corresponds to 18,861 nodes (2256 nodes for the die and 16,605 for the tube).

The workpiece material is defined as an elastic-plastic behavior using Young's modulus E, density ρ, and Poisson's ratio υ as presented in an earlier section. The strain isotropic hardening is described using several points outcome from the true tensile stress versus plastic strain over the yield strength and below the tensile strength. In order to simplify the simulation answer, the tube material is supposed to be isotropic.

Boundary conditions and contact definition

During the first step of the THF process (Figure 4), the die is embedded on its reference point since rigid motion is always represented on the reference point as reported by Zhao et al.,[26] whereas the tube is constrained to translate along the global X-axis, Y-axis, and Z-axis respectively in (yz), (xz), and (xy) surfaces to ensure the symmetry conditions. In addition, a pressure of 28 MPa is applied to the tube inner surface. In the second step of this simulation, all the boundary conditions applied in the first step remain

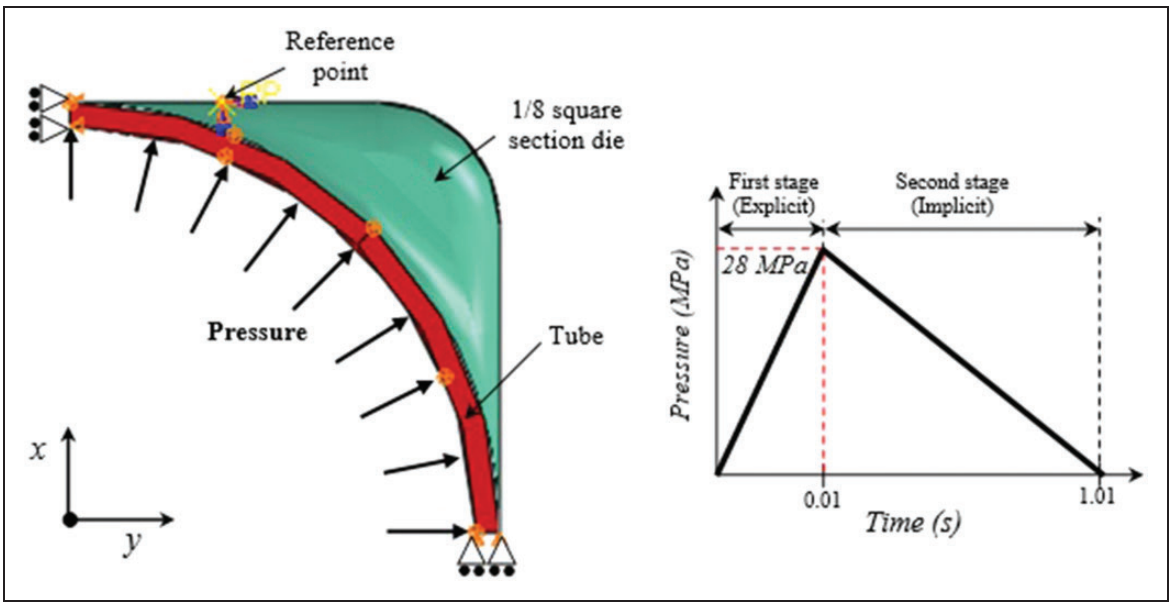

Figure 4. Applied load and boundary conditions.

identical except the pressure value that change to zero (i.e. the die–tube contact equivalent forces are proportionally reduced to zero[27]).

The contact between the die and the tube outer surface under dry condition is modeled, for the two steps (stages), by a master–slave contact approach using the "finite sliding" formulation, which gives the possibility of separation between the two surfaces during sliding. The friction coefficient on the contact surfaces meets Coulomb friction law and it is assumed to be constant during the THF process. This formulation provides accurate results with just one input parameter, which is Coulomb friction coefficient penalty. A literature review has shown that the COF in hydroforming process, under similar studied dry conditions, varies from 0.075 to 0.1.[28] Consequently, the COF is assumed equal to 0.1 in this FE validation part.

In the studied process, it is impractical to run the metal-forming analysis in its physical time scale using the dynamic explicit approach since the computation time would be very large. Increasing artificially the density of the material by adding some "nonphysical" mass that is called mass scaling is an effective method for increasing the stability limit and minimizing the computation time. However, high values of the mass scaling increases the kinetic energy of the moving mass. Indeed, to obtain reasonable results the mass scaling should be carefully chosen. In the present work, the optimal mass scaling factor, with a value of 100, was selected to run FE computations.

3D FE model validation

In order to validate the FE model, a set of numerical simulations are carried out. The numerical results obtained under a friction coefficient of 0.1 were compared with the experimental ones. Figure 5 shows that the thickness change along the cross-section of the hydroformed tube, performed with FE computation, is in good agreement with the experimental results. The average error between numerical and experimental results corresponds to 0.92% and 10.02% for the value and the position of the minimal thickness, respectively. Consequently, the proposed FE model can correctly predict the tube wall thickness along its cross-section length.

FE simulations reveal also the presence of a quasi-uniform thickness at the corner zone of the hydroformed tube. This result is in accordance with those found by Hwang and Chen[11] and Kridli et al.[29] when they have studied the THF process in a square die with the FE method. These authors have shown that the thickness variation in tubes, made up respectively of aluminum *AA6063-T4* and copper alloy *C12200*, appears to be constant at the corner zone in which the expansion is free.

In addition, to validate the FE model, both the internal pressure and the tube deformation are monitored by means of two displacement sensors placed at 120° of each other during the hydroforming process (Figure 6). This permits to plot a pressure–height expansion curve for the considered displacement sensor. In this case, only the first sensor (sensor 1) is considered to follow the deformation during expansion test (i.e. sensor 2 gives the same displacement than sensor 1). The comparison between experimental and numerical displacement of the tube outer surface near sensor 1 zone, shows that maximal deviation is observed in a pressure range from 15 to 21 MPa in which the error does not exceed 10%. However, the error measured at the end of the process remains less than 1.6%.

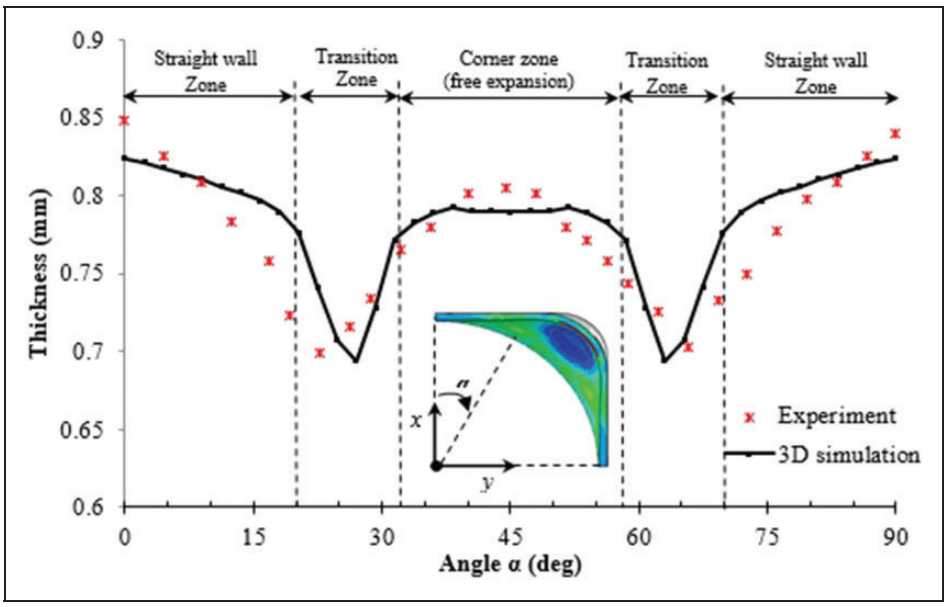

Figure 5. Thickness distribution along the tube cross section (FE simulations vs. experiment).

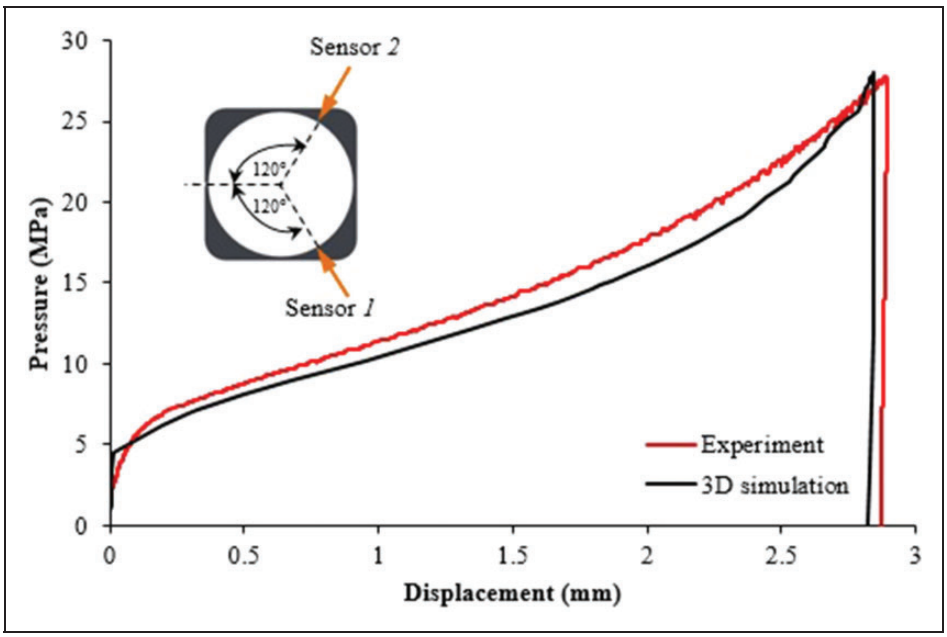

Figure 6. Evolution of the internal pressure against the displacement (sensor 2) in a square section die.

Finally, it is clear from the above that the FE model is valid and can be exploited to study the effect of the friction coefficient in plastic flow and residual stresses along the tube during and after hydroforming process.

Results and discussions

In term of product design, two main objectives should be taken into account. They consist of reducing the spring-back effects and minimizing the excessive thinning on the shaped tube in order to minimizing geometrical errors and maintain uniform thickness respectively. Then, to guarantee a suitable functioning of the hydroformed part the product must be free from cracks or wall failures. In addition, the residual stresses should be controlled to avoid post production annealing processes. Indeed, all these studied parameters will be discussed later as function of friction coefficient and die–tube contact conditions.

Effect of the COF and the relative die–tube slip distribution on the tube thickness distribution

Numerous numerical simulations have been carried out with different COFs to study the effect of this parameter on the THF process. The obtained results (Figure 7) show that this coefficient can affect

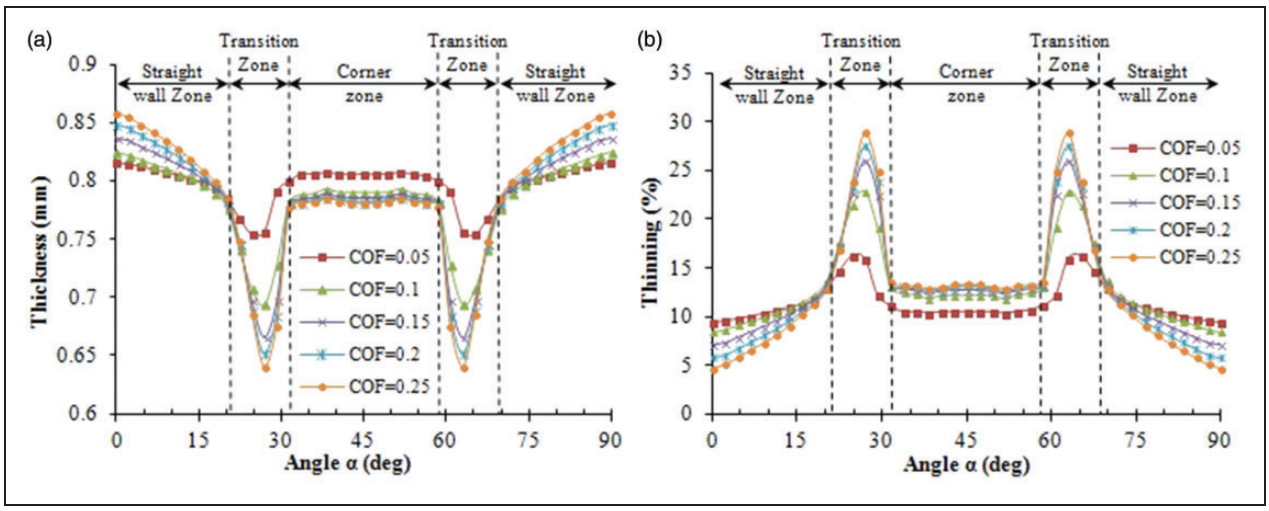

Figure 7. Effect of friction coefficients on: (a) tube thickness and (b) thinning distribution along the tube cross section with different COFs.

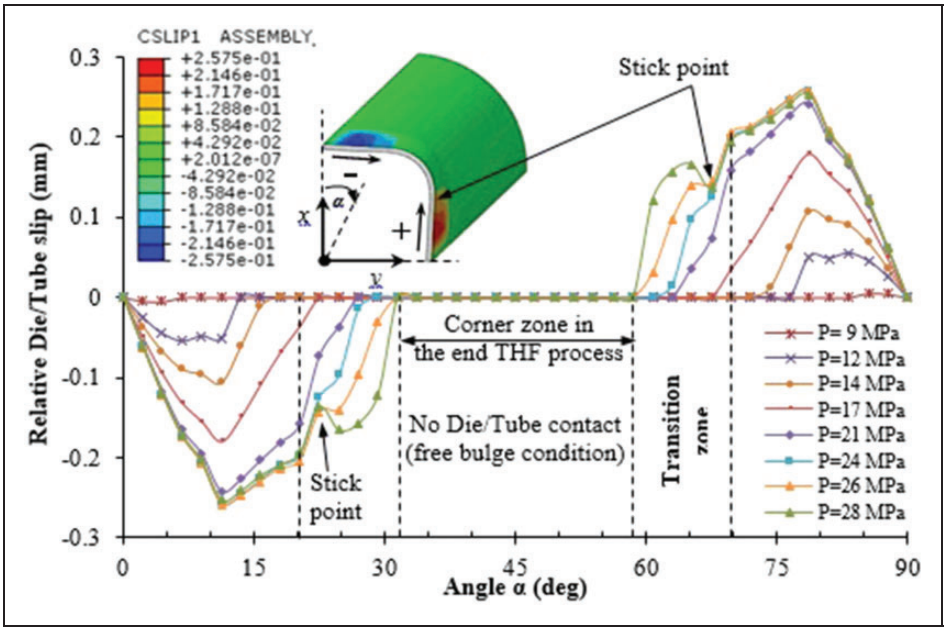

Figure 8. Relative die–tube slip distribution along tube cross section length during the THF process (COF = 0.1, pressure varies from 0 to 28 MPa).

considerably the thickness values along the tube cross-section. Three different zones can be clearly distinguished: straight wall, transition zone, and corner radius (free expansion zone). It is clear that the smallest thickness (Figure 7(a)) (maximum of thinning values (Figure 7(b)) was observed in the transition zone for all studied COFs.

Ngaile et al.[30] demonstrated when they studied the effect of the friction coefficient in a THF process, for both T-shape and limiting dome height test, the presence of these three different zones. Furthermore, they have shown that the difference in the material flow and the state of stress can expose these zones to different friction conditions that vary along the tube straight wall zone. Since the friction is directly related to the normal pressure applied into the surface, by increasing the forming pressure, friction between the tube and the die prevents the material flow. Figure 8 shows that relative die–tube slip goes through a maximum (minimum) approximately in the middle of the straight wall zones. When the applied pressure during the THF process grows higher than 24 MPa, the relative slip remains quasi-constant in the region of the stick point. The change in the contact conditions from stable sliding to stick-slip, which take place in the transition zone, can be the principle cause of the excessive tube thinning obtained in this zone. Hence, the higher friction generated in the die–tube contact area appears to be the cause of the additional thinning observed in the tube transition zone

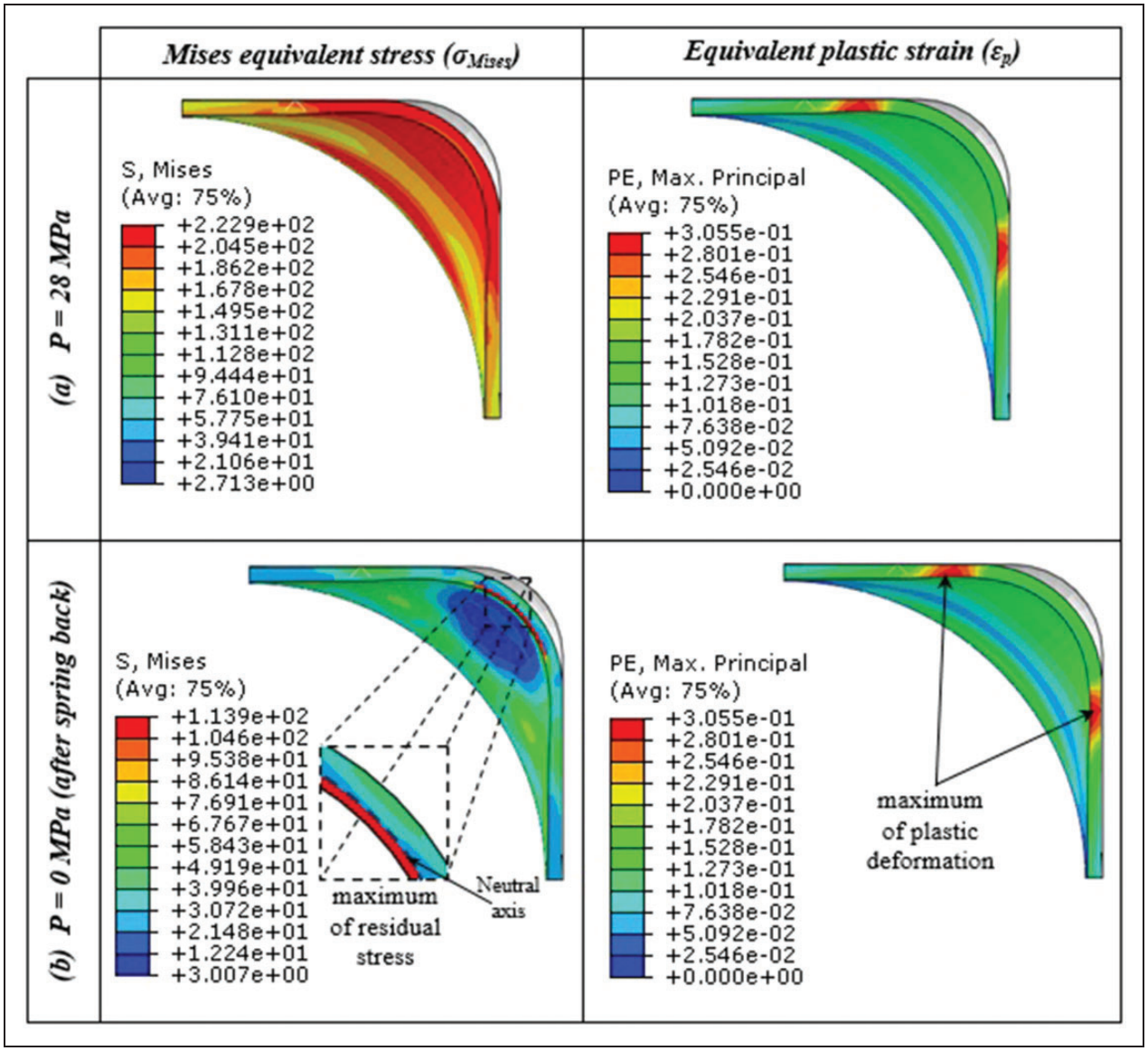

Figure 9. Residual stress and plastic strain distribution on the hydroformed tube before and after springback (COF = 0.15).

(thinning values varies from 16% to 28.9% when COF changes from 0.05 to 0.25, respectively; Figure 7(b)). This reduces the possibility for application of further pressure to achieve sharper corners.

Assessment of the COF effect on plastic deformation and residual stresses

To achieve a successful THF process, some parameters need be appropriately controlled in terms of material behavior and lubrication conditions. These parameters can affect the plastic deformation and residual stress repartition of the hydroformed tubes. Uniform thickness distribution and low residual stresses are suitable for most formed parts. Figure 9 shows the distribution of von Mises equivalent stress and the plastic strain throughout the tube before and after the tube spring-back. At the beginning of the first stage of the THF operation, the equivalent von Mises stress is uniformly distributed throughout the square section until the material yields stress value. With higher internal pressure (28 MPa; Figure 9(a)), the equivalent stress increases and presents higher values near the transition and the corner zones, whereas the plastic strain appears to be confined around the transition zones. These results are consistent with those reported earlier by Cui et al.[31] in their work about the deformation of double-sided THF, made of 5A02-O aluminum alloy, in square die.

At the end of the THF process (Figure 9(b)), it is observed that the values of residual stresses are more important near the inner surface in the corner zone (up to 110 MPa) compared to the outer side. In addition, the plastic strain values seem to be invariable in the corner zone due to the negligible contribution of elastic strain part to the total strain at large strain domain.

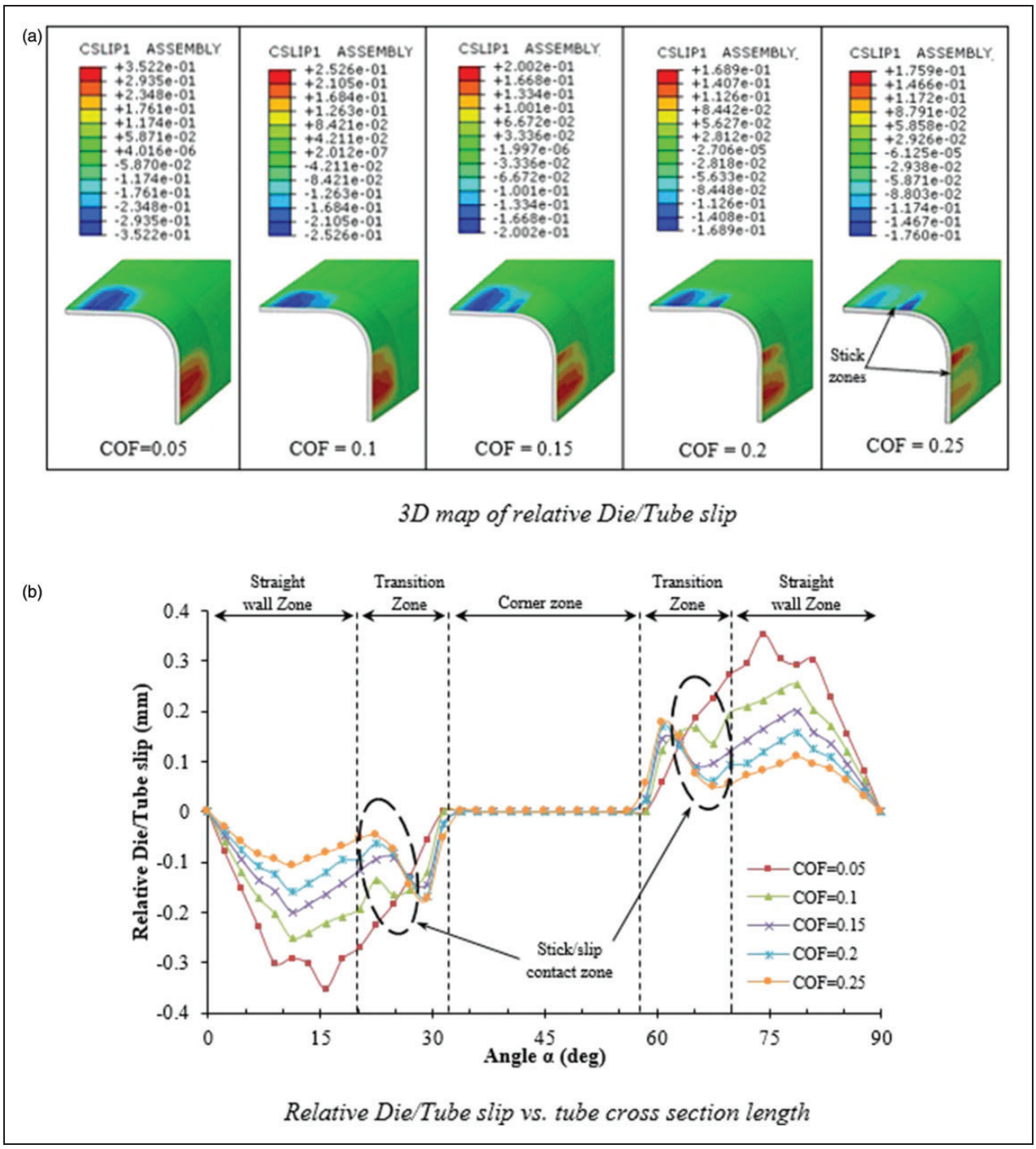

Figure 10. Relative die–tube slip in the end of the THF process at different COF values.

Figure 9(b) shows that the neutral axis in the corner zone is shifted to the inner surface. The neutral axis is defined as the axis in the cross-section of a beam along which there are no longitudinal stresses or strains. The neutral axis generally located in the middle between inner and outer surfaces, in a bending process, can be shifted to the inner surface when the tube corner radius-to-thickness (r/t) ratio decrease.[32,33] The identification of the repositioned neutral axis location in the tube after hydroforming process is essential since it permits to identify the area within the tube under tensile (expansion) and compressive (compressed) stresses. The influence of neutral axis position in the plastic deformation and residual stress will be discussed later with more details.

In addition, in order to study the evolution of the residual stresses and plastic strain along the cross-section of hydroformed tube it is crucial to examine the evolution of die–tube contact conditions with the process parameters. The relative die–tube slip in the end of the THF process is presented in Figure 10 with

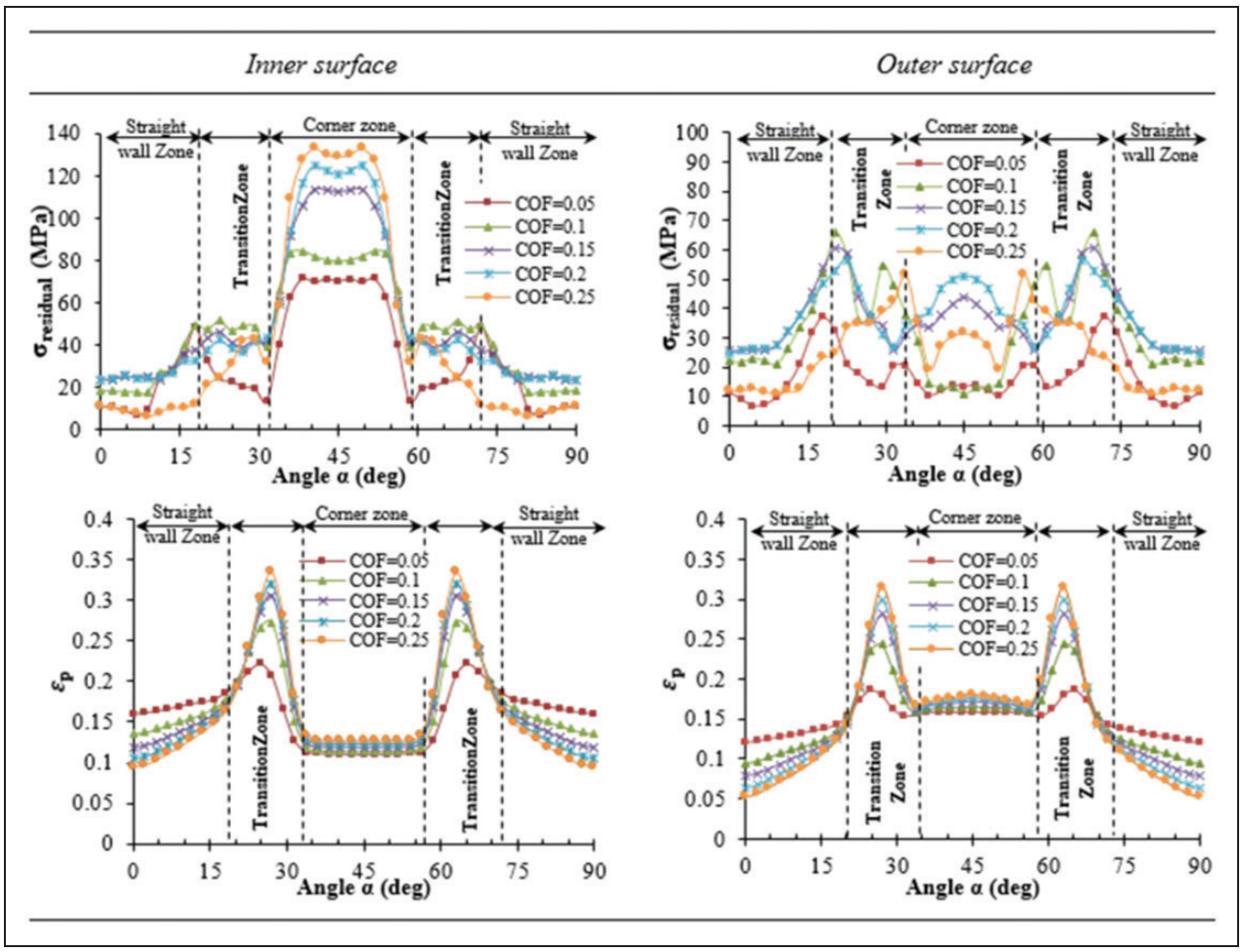

Figure 11. Distribution of residual stress ($\sigma_{residual}$) and plastic strain (ε_p) in the tube cross-section after hydroforming process.

different COF values. It is clear that die–tube slip region appears as a continued compact zone for the lowest value of the studied friction coefficient (COF = 0.05). Nevertheless, for higher COF values, it seems that die–tube slip regions present two adjacent slip zones separated by a third one that corresponds to the stick zone (the relative die–tube slip goes through a local minima). The evolution of relative die–tube slip values along the hydroformed tube cross-section (Figure 10(b)) shows, as found in the previous section, that the stick zone seems to play an important role in the tube plastic flow. This change in contact condition can limit the maximal thinning zone at the border between the straight wall zone and the corner zone for all studied COF.

Finally, the subsequent residual stresses and plastic strain along the cross-section are discussed in the section with more details by correlating the problem with mechanisms involved in the studied hydroforming process. The residual stresses and plastic strain evolution on both inner and outer tube surfaces are depicted in Figure 11.

The plastic strain values in the straight wall zone are slightly lower in the outer surface compared to the inner one. This can be explained first by the fact that die–tube friction can slightly reduce the material flow in this zone. This phenomenon became more pronounced when the COF values increase. In addition, it can furthermore be explained by the flattering of the circular tube during the THF process, which is close to the bending process (i.e. the outer surface layer contracts and the inner layer expands). Indeed, both frictional and bending effects can lead to the larger plastic strain observed on the inner surface of the straight well zone. Nevertheless, the values of plastic strain, in the corner zone, seem to be independent of the studied COF values. This can be explained by the fact that the corner zone was deformed only under the free bulge conditions. The slight upper values of plastic deformation observed in the outer surface ($0.158 \leq \varepsilon_p \leq 0.179$) compared to the inner surface ($0.114 \leq \varepsilon_p \leq 0.126$), in the corner zone, can be attributed to the shift of the neutral axis to the inner surface as shown above (i.e. r/t ratio is relatively small). This result is in close agreement with the analytical results found by Chinnaraj and Ramasamy[32,33] when they studied the effect of shift neutral axis on formed plastic strain and residual stresses in cold-formed steel with the assumption of elastic-perfectly plastic material model.

The studied tube, obtained by hydroforming process, is typically accompanied with an elastic spring back, which largely occurs in the corner sections. The main reason for the elastic spring back is the presence of small elastic region during plastic deformation, which has a tendency to recover to its original shape. Due to the partial elastic recovery and the unrecovered elasticity working against a permanently set plastic deformation, the resulting residual stress manifests as a nonlinear through-thickness in the direction of tube cross-section bending. This occurs in the absence of any external loads. Figure 11 shows the evolution of residual stresses, in both inner and outer surfaces along the tube cross-section for different COF values. The first examination of residual stresses subfigures show a nonsignificant difference between both inner and outer surface in the straight wall zone. This difference appears very small in the transition zone due to the effect of die–tube friction on the outer surface. However, it became more important in the corner zone. The residual stresses are always higher near the inner thickness of corner sections than the outer surface. This result is principally explained by the shift of the tube neutral axis, in the corner zone, from the middle tube thickness to the inner axis due to the small value of r/t ratio. This result is also in a good agreement with the analytical results found by Chinnaraj and Ramasamy.[32,33] In addition, it is clear that the COF affects significantly the values of the residual stresses principally in the corner zone (Figure 11). The maximum values of residual stresses vary from 71 MPa to 132 MPa when the COF value increases from 0.05 to 0.25, respectively. As a result, it is clear that both die–tube friction conditions and the tube bending effects, which occur respectively in the tube straight wall and corners zones, are the principal causes of the obtained residual stresses distribution along the tube cross-section. This confirms that a good lubrication can reduce not only the maximum thinning but also the residual stresses.[34]

Conclusion

The work presented in this manuscript is based on a 3D-FE analysis of THF process in a square section die to study the material plastic flow and to predict residual stresses induced in tube after the spring-back phenomenon. Based on the obtained results, the following conclusions can be drawn:

- A comparative study between the FE model and the experimental measurements has shown a good correlation in prediction of (i) the location and the value of the maximal thinning and (ii) the tube corner displacement measured via a sensor. As a result, the FE model was validated and retained to study the effect of friction coefficients on the die–tube contact condition and its effects on plastic flow and residual stresses.
- Three different zones can be clearly distinguished: straight wall, transition zone, and corner radius (free expansion zone). It is obvious that the smallest thickness (maximum of thinning values) was observed in the transition zone for all studied COFs.
- The difference in the material flow and the state of stress can expose these zones to different friction conditions, which vary around the edge situated between the tube straight wall and the corner zone. Since the friction is directly related to the normal pressure applied on to the surface, friction between the tube and the die prevent the material flow especially around the stick point located in the transition zone, which can be the major cause of the excessive tube thinning obtained in this zone.
- The evolution of the plastic strain on both inner and outer surfaces presents the same tendencies. In addition, the values of plastic strain in the corner zone seems to be quasi-uniform since the corner zone is deformed under free bulge mechanical condition independently of different COF values. In addition, the slight upper values of plastic deformation observed in outer surface compared to the inner, still in the corner zone, are attributed to the shift of the neutral axis to the inner surface.
- The residual stresses are higher near the inner thickness of corner sections than the outer surface. This result is mainly explained by the shift of the tube neutral axis, in the corner zone, from the middle tube thickness to the inner axis due to the small value of r/t ratio. In addition, it is clear that the COF affects significantly the values of the residual stresses particularly near the outer surface of the tube corner zone.

Acknowledgments

The authors would like to thank Ms Fardi Hayet, engineer in SEGULA Technologies, Mr Gerard Michel, research-engineer at the FEMTO-ST lab, and Dr Ludovic Vitu, for their helps and contribution to this research.

Declaration of conflicting interests

The author(s) declared no potential conflicts of interest with respect to the research, authorship, and/or publication of this article.

Funding

The author(s) disclosed receipt of the following financial support for the research, authorship, and/or publication of this article: This study was funded by the FEMTO-ST lab.

ORCID iDs

A Ktari https://orcid.org/0000-0002-2731-0717
N Guermazi https://orcid.org/0000-0002-3666-7152

References

1. Alaswad A, Benyounis KY and Olabi AG. Tube hydroforming process: a reference guide. *Mater Des* 2012; 33: 328–339.
2. Koç M and Cora ON. *Hydroforming for advanced manufacturing*. Cambridge: Woodhead Publishing Ltd, 2008.
3. Ahmed M and Hashmi MSJ. Comparison of free and restrained bulge forming by finite element method simulation. *J Mater Process Technol* 1997; 63: 651–654.
4. Koç M and Altan T. An overall review of the tube hydroforming (THF) technology. *J Mater Process Technol* 2001; 108: 384–393.
5. Li S, Xu X, Zhang W, et al. Study on the crushing and hydroforming processes of tubes in a trapezoid-sectional die. *Int J Adv Manuf Technol* 2009; 43: 67–77.
6. Abdelkefi A, Malécot P, Boudeau N, et al. On the tube hydroforming process using rectangular, trapezoidal, and trapezoid-sectional dies: modeling and experiments. *Int J Adv Manuf Technol* 2017; 93: 1725–1735.
7. Vollertsen F and Plancak M. On possibilities for the determination of the coefficient of friction in hydroforming of tubes. *J Mater Process Technol* 2002; 125: 412–420.
8. Manabe KI and Amino M. Effects of process parameters and material properties on deformation process in tube hydroforming. *J Mater Process Technol* 2002; 123: 285–291.
9. Fuchizawa S. Influence of strain-hardening exponent on the deformation of thin-walled tube of finite length subjected to hydrostatic internal pressure. *Adv Technol Plast* 1984; 1: 297–302.
10. Khalfallah A, Zribi T and Belhadjsalah H. Application of tube hydroforming in square cross-section die for inverse identification method validation. *Key Eng Mater* 2013; 554: 966–973.
11. Hwang YM and Chen WC. Analysis of tube hydroforming in a square cross-sectional die. *Int J Plast* 2005; 21: 1815–1833.
12. Geiger M, Dal Bó P and Hecht J. Improvement of formability in tube hydroforming by reduction of friction with a high viscous fluid flow. *Int J Adv Mater Res* 2005; 6: 369–376.
13. Fiorentino A, Ceretti E, Attanasio A, et al. Experimental study of lubrication influence in the production of hydroformed T-joint tubes. *Key Eng Mater* 2009; 410: 15–24.
14. Yuan SJ, Han C and Wang XS. Hydroforming of automotive structural components with rectangular-sections. *Int J Mach Tool Manuf* 2006; 46: 1201–1206.
15. Chen FK, Wang SJ and Lin A. Study of forming pressure in the tube-hydroforming process. *J Mater Process Technol* 2007; 192: 404–409.
16. Nikhare C, Weiss M and Hodgson PD. FEA comparison of high and low pressure tube hydroforming of TRIP steel. *Comput Mater Sci* 2009; 47: 146–152.
17. Yangui W, Ktari A, Gammoudi M et al. Sheet metal forming in the case of hinge manufacturing process, Part 2: numerical study. *Int J Adv Manuf. Technol* 2018; 95: 367–374.
18. Laredj M, Miloudi A, Lousdad A, et al. Prediction and optimizing residual stress profile induced by cold expansion in aluminum alloys using experimental design. *Fract Struct Integr* 2019; 48: 193–207.
19. Abdelkefi A, Guermazi N, Boudeau N, et al. Effect of the lubrication between the tube and the die on the corner filling when hydroforming of different cross-sectional shapes. *Int J Adv Manuf Technol* 2016; 87: 1169–1187.
20. Ranta-Eskola AJ. Use of the hydraulic bulge test in biaxial tensile testing. *Int J Mech Sci* 1979; 21: 457–465.
21. Zribi T, Khalfallah A and BelHadj SH. Experimental characterization and inverse constitutive parameters identification of tubular materials for tube hydroforming process. *Mater Des* 2013; 49: 866–877.
22. Boudeau N and Malécot P. A simplified analytical model for post-processing experimental results from tube bulging test: theory, experimentations, simulations. *Int J Mech Sci* 2012; 65: 1–11.
23. Ktari A, Antar Z, Haddar N, et al. Modeling and computation of the three-roller bending process of steel sheets. *J Mech Sci Technol* 2012; 26: 123–128.
24. Song F, Yang H, Li H, et al. Springback prediction of thick-walled high-strength titanium tube bending. *Chin J Aeronaut* 2013; 26: 1336–1345.
25. Meinders T, Burchitz IA, Bonte MHA, et al. Numerical product design: springback prediction, compensation and optimization. *Int J Mach Tools Manuf* 2008; 48: 499–514.
26. Zhao GY, Liu YL, Yang H, et al. Three-dimensional finite-elements modeling and simulation of rotary-draw bending process for thin-walled rectangular tube. *Mater Sci Eng A* 2009; 499: 257–261.
27. Li KP, Carden WP and Wagoner RH. Simulation of springback. *Int J Mech Sci* 2002; 44: 103–122.
28. Crapps J, Marin EB, Horstemeyera MF, et al. Internal state variable plasticity-damage modeling of the copper tee-shaped tube hydroforming process. *J Mater Process Technol* 2010; 210: 1726–1737.
29. Kridli GT, Bao L, Mallick K, et al. Investigation of thickness variation and corner filling in tube hydroforming. *J Mater Process Technol* 2003; 133: 287–296.
30. Ngaile G, Jaeger S and Altan T. Lubrication in tube hydroforming (THF): Part II. Performance evaluation of lubricants using LDH test and pear-shaped tube expansion test. *J Mater Process Technol* 2004; 146: 116–123.
31. Cui X-L, Wang X-S and Yuan S-J. Deformation analysis of double-sided tube hydroforming in square-section die. *J Mater Process Technol* 2014; 214: 1341–1351.
32. Chinnaraj, K. and Padmanaban, R. Analytical prediction of residual stresses in cold formed steel sections with elastic-perfectly plastic material model. SAE Paper 2017-26-0169, 2017.
33. Chinnaraj K, Sathya Prasad M, Lakshmana Rao C, et al. Investigation of residual stresses in cold-formed steel sections with nonlinear strain-hardened material model. *Int J Mater Manuf* 2018; 11: 229–240.
34. Bruni C, Celeghini M, Geiger M, et al. A study of techniques in the evaluation of springback and residual stress in hydroforming. *Int J Adv Manuf Technol* 2007; 33: 929–939.